

Analysis of the vibrational spectrum of the dihydrogen complex $[W(CO)_3(\eta^2-H_2)(P\{iso-propyl\}_3)_2]$: A model for the vibrational spectrum of dihydrogen surface species

Stewart F. Parker^{1*}, Anibal J. Ramirez-Cuesta¹, John Tomkinson¹
and Philip C.H. Mitchell²

¹ISIS Facility, The Rutherford Appleton Laboratory, Chilton, OX11 0QX, UK.

²School of Chemistry, University of Reading, Reading, RG6 6AD, UK.

Received: 18-09-05 Accepted: 26-10-05

Abstract

We have investigated the vibrational spectrum of the dihydrogen complex $[W(CO)_3(\eta^2-H_2)(P\{isopropyl\}_3)_2]$ with particular emphasis on the inelastic neutron scattering spectrum. Previous work treated the motion of the dihydrogen ligand as either the rotational transitions of dihydrogen in a deep attractive well or as the modes of a dihydrogen complex. We have shown that neither model on its own can account for the inelastic neutron scattering spectrum. The rotational model requires the addition of vibrations and the vibrational model, as calculated by density functional theory, requires the addition of a split ground state. We have also shown that there is significant mechanical coupling of the dihydrogen modes to those of the other ligands, especially the carbonyls. Simulation of the method used in the literature, shows that the most important result, the location of the torsional mode, is validated, but that the method is not reliable for higher energy modes. Assignments for the carbonyl modes and some of the skeletal modes are also given. The implications of the vibrational coupling for the use of the dihydrogen complexes as model compounds for surface species are considered.

Key words: Density functional theory; dihydrogen complex; inelastic neutron scattering; vibrational spectroscopy.

Análisis del espectro vibracional del complejo de di-hidrógeno $[W(CO)_3(\eta^2-H_2)(P\{isopropil\}_3)_2]$: Un modelo para el espectro vibracional de la especie de superficies dihidrógeno

Resumen

En esta comunicacion presentamos los resultados de la investigacion del espectro vibracional del compuesto de dihidrogeno $[W(CO)_3(\eta^2-H_2)(P\{isopropil\}_3)_2]$ poniendo enfasis en particular en el espectro inelastico de neutrones. En trabajos anteriores se ha tratado el movimiento del ligando de di-hidrogeno tanto como transiciones rotacionales de la molecula de hidrogeno

* Autor para la correspondencia. E-mail: s.f.parker@rl.ac.uk

en un pozo de potencial atractivo o como una serie de modos del complejo de di-hidrogeno. Nosotros demostramos que ninguno de estos modelos, por su propia cuenta, puede explicar el espectro inelastico de neutrones observado. El modelo rotacional requiere la presencia de vibraciones y el modelo vibracional, calculado mediante el uso de calculos ab-initio DFT (siglas en ingles de la teoria del funcional de la densidad) necesita la incorporacion de un estado base bifurcado. Tambien hemos demostrado que hay un acoplamiento significativo de los modos del dihidrogeno con los demas ligandos, especialmente los carbonilos. Simulaciones de los metodos utilizados en la literatura muestran que el resultado mas importante, la ubicacion de los modos torcionales es valida, pero que el metodo no es apropiado para los modos de mas alta energia. Asimismo presentamos las determinaciones de los modos de los grupos carbonil y esqueletales. Finalmente analizamos las consecuencias del acoplamiento vibracional en el uso de los compuestos de di-hidrogeno como modelos de moléculas adsorbida sobre superficies.

Palabras clave: Complejo de dihidrógeno; difracción de neutrones inelásticos; espectroscopía vibracional; teoría del funcional de la densidad.

Introduction

In the passage from physisorbed dihydrogen to chemisorbed hydride on a catalyst surface, there must be a stage where dihydrogen is bound to the active centre but the H-H bond is still present. For many years it was believed that this was a transition state, so could not be trapped and studied. This changed in 1984 with the announcement of a series of complexes that contained a sideways-on, η^2 -bound, dihydrogen ligand (1). The history of their discovery and a comprehensive review have been given (2).

The bonding in a dihydrogen complex is similar to the Dewar-Chat-Duncanson description (3) of bonding in an organometallic complex, viz. donation from a filled bonding orbital of the ligand to empty d -orbitals of the metal, and back donation from filled d -orbitals to empty non-bonding or antibonding orbitals of the ligand. Dihydrogen is unique in that back donation occurs to the empty σ^* -antibonding orbital of the dihydrogen ligand rather than to a π^* orbital. Both σ -donation from, and back donation to, dihydrogen causes weakening of the H-H bond, the bond length increasing from 0.746 Å, the value for gaseous dihydrogen, to, typically, 0.8 – 1.0 Å for a dihydrogen complex, although 'super-stretched' bond

lengths of 1.1 – 1.5 Å are known (4). The increase in bond length also requires that the observed (i.e. anharmonic) vibrational frequency of free dihydrogen, ν_{H-H} , (4159 cm^{-1}) should fall when dihydrogen is bound: values in the range 2000 – 3200 cm^{-1} are known, although 2600 – 3000 cm^{-1} is more typical (2).

The complexes serve as model compounds for an intermediate in the dissociative adsorption of hydrogen, as such, they provide a bridge between physisorbed and dissociated states of hydrogen. Their vibrational spectra can be used to characterise the complexes and provide information as to the modes that may be useful to identify dihydrogen intermediates on a surface. The complexes can be viewed from two directions: as an example of dihydrogen rotating in a strong potential, the rotational model, or as a conventional complex, the vibrational model. Since both viewpoints are describing the same phenomenon they should be equivalent. However, we shall see that both models are incomplete.

Experimental

The *ab initio* calculations were carried out using density functional theory (DFT) with the B3LYP hybrid functional and the

LanL2DZ basis set as implemented in Gaussian03 (5). The initial geometry was obtained from the crystal structure (1). The calculation reproduces the observed geometry very well apart from an overestimation in the W-H distance, Table 1. The vibrational spectra were then calculated from the energy minimised structure. The GaussView 3.0 package was used for visualisation of the modes. The Gaussian03 output includes the infrared and Raman intensities as well as the atomic displacements of all the atoms in each vibrational mode.

Inelastic Neutron Scattering

Inelastic neutron scattering is a form of vibrational spectroscopy. The major difference between inelastic neutron scattering (INS) spectroscopy and infrared and Raman spectroscopies is that the intensity of a transition is given by: (6)

$$S(Q, \omega)_l^n = \frac{\sigma_l}{4\pi} \frac{[Q^v u_l]^2 n}{n!} \exp\left(-\left(Q \sum_v v u_l\right)^2\right) \quad [1]$$

where $v u_l$ is the amplitude of vibration of atom l in the v th mode at energy ω , and momentum transfer Q with cross section σ_l . n is the order of the transition, $n = 1$ for a fundamental, $n = 2$ for a first overtone or binary combination and so forth. The dependence

on the cross section, means that scattering from hydrogen will dominate the spectrum since $\sigma_H = 82$ barn ($1 \text{ barn} = 10^{-28} \text{ m}^2$), all the other atoms present have $\sigma_l < 8$ barn. This includes deuterium ($\sigma_D = 7.6$ barn), since the cross section is both element and isotope dependent. Further, from equation (1) it can be seen that the scattering is purely dynamic; all that is needed to calculate an INS spectrum are the mode frequencies and the displacements of the atoms in the mode. These are provided by the Gaussian03 output and the programme ACLIMAX (7) was used to generate the INS spectrum from the *ab initio* output.

Results and Discussion

Dihydrogen rotating in a strong potential

The energy levels of the rigid rotor in free space are given by: (8)

$$E_{JM} = E_J = J(J+1) \frac{\hbar^2}{2I} = J(J+1) B_{\text{rot}} \quad [2]$$

where I is the moment of inertia of the molecule and B_{rot} is the rotational constant. For dihydrogen:

Table 1
Comparison of calculated and observed geometry of $[\text{W}(\text{CO})_3(\text{H}_2)(\text{P}(\text{isopropyl})_3)_2]$

	DFT	Experimental ¹
H-H / Å	0.82	0.84
W-H / Å	1.94, 1.94	1.75, 1.75
W-CO _{eq} / Å	2.01, 2.01	2.00, 2.00
W-CO _{ax} / Å	1.95	1.96
W-P / Å	2.60, 2.60	2.64, 2.45
H-W-CO _{eq} / °	87.8, 89.1	86.8, 89.5
H-W-CO _{ax} / °	167.8	168.7
H-W-P / °	77.1, 101.4	77.7, 102.7

$$I_{HH} = 2 \left(\frac{r_{HH}}{2} \right)^2 m = \mu r_{HH}^2 \quad [3]$$

$$B_{rot}^{HH} = \frac{\hbar^2}{2I_{HH}} \quad [4]$$

where r_{HH} is the dihydrogen bond length and μ is the reduced mass. The integers J and M are the angular momentum quantum numbers, with allowed values:

$$J = 0, 1, 2, \dots; M = 0, \pm 1, \pm 2, \dots \pm J \quad [5]$$

The magnetic quantum number, M , reflects the quantised nature of the z -components of the angular rotational momentum vector. In the gas phase the molecule is in an isotropic, zero valued, potential field and the relative orientations of the z -components are irrelevant. The number of orientations represents the total degeneracy of the J^{th} rotational state. The energy of the gas-phase molecule does not depend on M and the magnetic quantum number is often omitted.

Quantum mechanical restrictions on the symmetry of the rotational wave function produce two molecular species for dihydrogen: ortho- and para-hydrogen. The hydrogen nucleus, a particle with half-integer spin, is a fermion. Its quantum mechanical description must obey Fermi statistics, as expressed through the Pauli principle. This imposes a symmetry requirement on molecular wavefunctions and forbids the occupation of certain states. The total wavefunction (spin + nuclear) must be antisymmetric with respect to exchange of nuclei.

The even values of J correspond to antisymmetric wavefunctions and must be combined with symmetric nuclear spin wavefunctions. The only allowed rotational states of spin paired, or antiparallel ($\uparrow \downarrow$), dihydrogen are thus those with, $J=0, 2, 4, \dots$. This defines *para-hydrogen*. There are $2J+1$ possible spin states for each acceptable J value and it follows from Eq. [2] that there is only

one spin state for the para-hydrogen ground state, $J=0$.

The odd rotational values of J correspond to symmetric rotational wavefunctions and, in order to have an antisymmetric total wavefunction, these must be combined with antisymmetric nuclear spin wavefunctions. The odd rotational states $J=1, 3, 5, \dots$ are combined with a symmetric nuclear spin wavefunction (where nuclear spins are parallel, or unpaired, $\uparrow \uparrow$). This defines *ortho-hydrogen* and again its degeneracy, in the gas phase, is the $2J+1$ possible spin states.

In Raman spectroscopy, but not in infrared spectroscopy, transitions within the spin manifolds are allowed with the selection rule $\Delta J = \pm 2$. In the absence of a catalyst, transitions between the spin paired and spin unpaired states are rare, the species are 'spin-trapped'. Dihydrogen is, therefore, effectively a mixture of two stable species, para-hydrogen and ortho-hydrogen, where the molecules mix freely and there is little exchange between the two populations. Transitions between the manifolds are observable by inelastic neutron scattering (INS) spectroscopy (6) since the neutron is a spin one-half particle.

Transitions within the separate para- or ortho-hydrogen manifolds are controlled by the *coherent cross section* of hydrogen, 1.76 barn, and these transitions are too weak to be observed in its INS spectrum. In contrast, spin-flip transitions, between the manifolds, are controlled by the *incoherent cross section* of hydrogen, 80.3 barn, and are readily observable by INS spectroscopy (9).

When dihydrogen is bound to a metal, the rotational model, the potential becomes anisotropic (the unique direction of the potential is taken to lie along the z -axis). A commonly used (10) expression for the potential that governs the rotation of the molecule is:

$$V(\theta, \phi) = \left[a + \frac{b}{2} \cos 2\phi \right] \sin^2 \theta \quad [6]$$

where θ is the polar angle (the angle between the H-H bond and the z-axis), ϕ is the azimuthal angle (between the x axis, defined in the plane normal to z, and the projection of the H-H bond onto this plane). The values of a and b give the relative weights of the potential and the factor two in 2ϕ represents how the symmetry of the field matches the C_2 molecular symmetry. Treating the orientational potential as a perturbation and expanding it in spherical harmonics, Y_{JM} , we can solve the Schrödinger equation for the system. The relevant Hamiltonian is:

$$H_{J' M' J M} = J(J+1)B_{\text{rot}} \delta_{J' J} \delta_{M' M} + \langle Y_{J' M'} | V(\theta, \phi) | Y_{J M} \rangle \quad [7]$$

where the primes denote the upper state. The resultant matrix is diagonalised numerically to determine the energy states of the perturbed rotor. A minimum of 64 rotational levels must be calculated to obtain an

error smaller than $B_{\text{rot}} \times 10^{-5}$ in the calculated energies. The energy levels are shown in Figure 1. Since most INS experiments involve para-hydrogen in its ground state, Figure 1 refers all energies to the energy of that state. Note that the absolute energy of the ground state actually rises as the potential deepens and the convention of Figure 1 is not universally followed in the literature. In particular, Eckert and co-workers (11, 12) use the energy of the unperturbed rigid rotor as the zero of energy, which explains why their graphs of energy versus potential differ from ours. The labels of the states refer to the unperturbed case since, strictly, J and M are no longer good quantum numbers in the presence of an external field.

For a dihydrogen complex, the appropriate model is that of a perturbed planar rotor in a deep attractive field. In this case both a and b are large so the potential is a waisted, figure-of-eight-like shape. This is chemically reasonable because the dihydrogen occupies a well-defined position in the

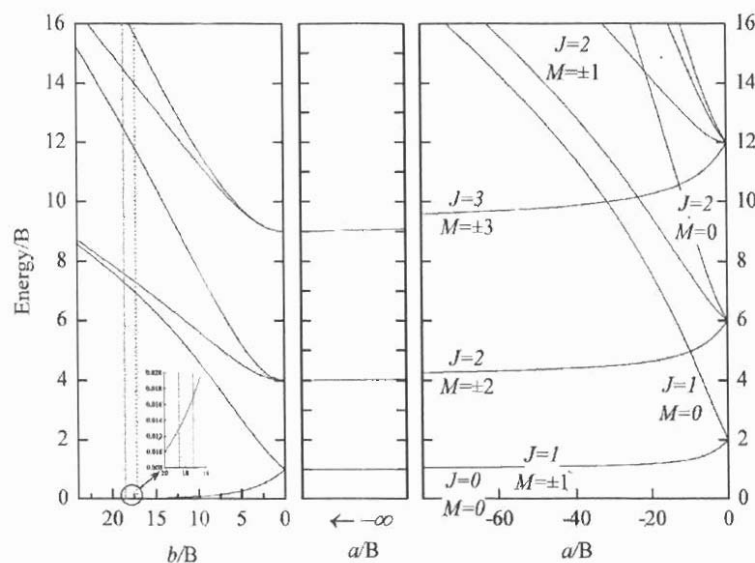


Figure 1. The energies of the rotational states of dihydrogen as a perturbed planar rotor in a deep attractive field. The dashed vertical line shows the transitions expected for $[W(CO)_3(H_2)(P\{isopropyl\}_3)_2]$ with tunnel splittings of 0.62 and 0.80 cm^{-1} (inset).

complex and the 'cups' of the potential give the hydrogen positions.

Transitions between all the levels are allowed but because the intensities of para-to-para- and ortho- to ortho- transitions depend on the (small) coherent cross section of hydrogen they will be unobservable in practice and only para- to ortho- or ortho- to para- transitions will be observed in the INS spectrum. Thus the expected transitions are: $\{J, M (1, 1 \leftarrow 0, 0)\}$, $\{J, M (1, +1 \leftarrow 0, 0)\}$, $\{J, M (2, -2 \leftarrow 1, -1)\}$, $\{J, M (2, +2 \leftarrow 1, -1)\}$ and $\{J, M (3, \pm 3 \leftarrow 0, 0)\}$.

From Figure 1, the lowest energy rotational transition, $\{J, M (1, -1 \leftarrow 0, 0)\}$ occurs in the energy regime expected for tunnelling transitions ($< 20 \text{ cm}^{-1}$). Even at very low temperature ($20 \text{ K} \sim 14 \text{ cm}^{-1}$) there will be a significant population of the (1, -1) level and this gives rise to the two transitions to the $J=2$ levels.

Thus the spectrum in the vibrational spectroscopy region ($> 100 \text{ cm}^{-1}$) would be expected to consist of four peaks (ignoring any contribution from the other ligands present). Transitions to higher J, M values will also occur but will be difficult to observe because of the effects of recoil and the Debye-Waller factor.

One of the first dihydrogen complexes to be discovered was $[W(CO)_3(\eta^2-H_2)(P\{isopropyl\})_3]$ (1). We have chosen to use this complex as an example because the crystal structure is known (1) and the phosphine ligands have fewer atoms than the corresponding cyclohexyl complexes. This makes the complex more tractable computationally.

There are 42 hydrogen atoms associated with the phosphines so these would dominate the INS spectrum. To avoid the difficulty and expense of preparing deuterated phosphines, the difference spectrum was used: the spectrum of the dideuterium complex was subtracted from that of the dihydrogen complex. The result is shown in Figure 2 (11).

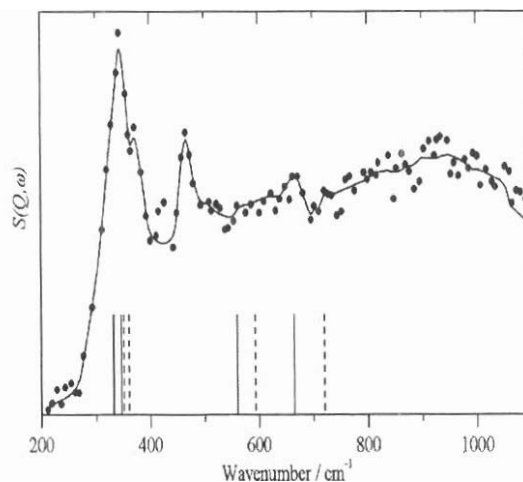


Figure 2. The difference INS spectrum of complexed dihydrogen recorded with the FDS spectrometer at LANSCE. The points are $[W(CO)_3(H_2)(P\{isopropyl\})_3] - [W(CO)_3(D_2)(P\{isopropyl\})_3]$. The vertical lines indicate the calculated positions of the dihydrogen rotational transitions having 0.62 cm^{-1} (solid line) and 0.80 cm^{-1} (dashed line) as the lowest energy transitions. Adapted from¹⁴ with permission from the American Chemical Society.

For this complex (1) $r_{HH} = 0.84 \text{ \AA}$ hence $r_{HH} = 47.4 \text{ cm}^{-1}$, Eq. [4], (cf. for gaseous H_2 , $r_{HH} = 0.746 \text{ \AA}$ and $B_{rot}^{HH} = 59.3 \text{ cm}^{-1}$). In this complex, one of the phosphine ligands is disordered, which gives rise to two slightly different barriers to rotation and hence two sets of transitions. The lowest transitions are at: (11) $0.62 (0.013 B)$ and $0.80 \text{ cm}^{-1} (0.017 B)$ so from Figure 1 transition energies of $346 (7.3 B)$, $360 (7.6 B)$, $592 (12.5 B)$ and $720 \text{ cm}^{-1} (15.2 B)$ for the 0.62 cm^{-1} set and $332 (7.0 B)$, $346 (7.3 B)$, $559 (11.8 B)$ and $664 \text{ cm}^{-1} (14.0 B)$ for the 0.80 cm^{-1} set are predicted and from Figure 2 four bands are apparent at $340, 370, 460$ and 660 cm^{-1} in qualitative agreement with the prediction.

Dihydrogen as a Ligand

The disadvantage of the dihydrogen-in-a-potential model is that it ignores all the vibrations of the coordinated dihydrogen except the torsion; it assigns the entire spectrum in terms of rotational transitions of dihydrogen.

The alternative is to consider dihydrogen as a ligand and to treat the vibrations of the dihydrogen in the conventional manner, the vibrational model. Gaseous dihydrogen has six degrees of freedom: one internal (the H-H stretch), two rotational and three translational. When bound, the rotational and translational degrees of freedom become frustrated and appear as internal modes of the complex as shown in Figure 3. It has proven extraordinarily difficult to observe all of the modes and only by using the combination of infrared, Raman and INS spectroscopies has it been feasible in two cases, those of $[\text{W}(\text{CO})_3(\text{H}_2)(\text{PR}_3)_2]$ (R = cyclohexyl, isopropyl) (11-14).

It is possible to test the validity of the vibrational model by calculating the vibrational spectra with DFT. Figure 4a shows the calculated INS spectrum of $[\text{W}(\text{CO})_3(\text{H}_2)(\text{P}[\text{isopropyl}]_2)_2]$. (The spectrum is

that that would be obtained with the high resolution INS spectrometer TOSCA (15) at ISIS, UK). The complexity of the INS spectrum is readily apparent hence the need for the difference technique. Figure 4b shows the same spectrum (with a $\times 10$ ordinate expansion) but with the cross sections of all the atoms except for the two hydrogen atoms in the dihydrogen ligand set to zero, *i.e.* only the modes involving dihydrogen motion contribute to the spectrum. It can be seen that there are many modes that involve significant dihydrogen motion.

The dihydrogen-only spectrum of Figure 4b is an idealised version of the experimental difference spectrum, Figure 2. The difference spectrum assumes that the dihydrogen (dideuterium) modes are not strongly coupled to those of the rest of the complex; if this is so, then the difference spectrum will contain only the dihydrogen modes. Figure 5 compares the experimental difference spectrum and a smoothed version of Figure 4b. The latter includes phonon wings, overtones and combinations to better represent the spectrum.

The smoothing is to reproduce the modest resolution of the INS spectrometer

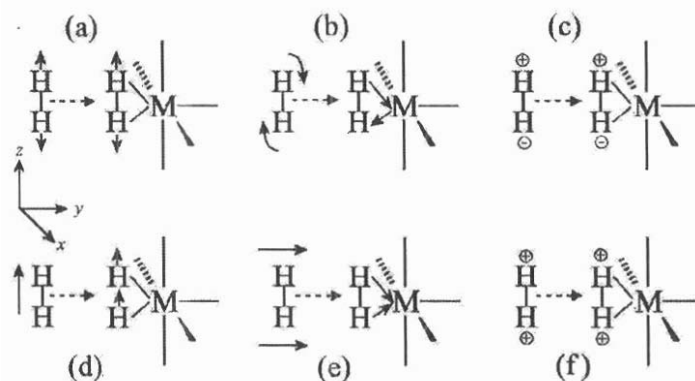


Figure 3. How the six degrees of freedom of free dihydrogen become six internal modes of vibration of an η^2 -coordinated dihydrogen molecule. (a) $\nu_{\text{HH}} \rightarrow \nu_{\text{HH}}$, (b) x axis rotation becomes the M-H₂ antisymmetric stretch (ν_{HMHasy}), (c) y axis rotation becomes the M-H₂ torsion, (d) z axis translation becomes the MH₂ rock, (e) y axis translation becomes the M-H₂ symmetric stretch (ν_{HMHsym}) and (f) x axis translation becomes the MH₂ wag.

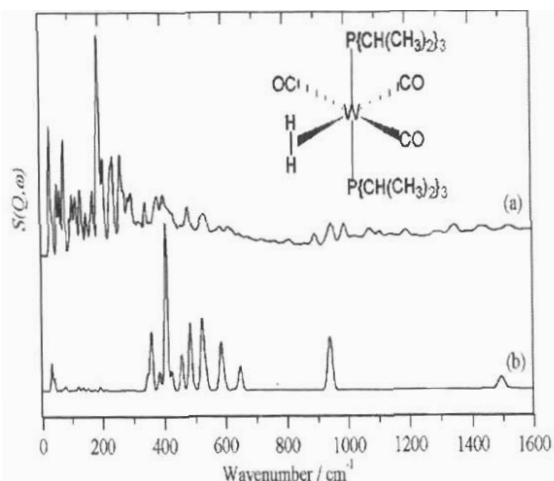


Figure 4. The INS spectrum of complexed dihydrogen, in $[W(CO)_3(\eta^2-H_2)(P(iso-propyl)_3)_2]$ calculated by DFT (B3LYP/LanL2DZL). (a) All atoms included and (b) only the dihydrogen ligand. Note that (b) is 10 ordinate expanded relative to (a) and only the fundamentals (without phonon wings) are plotted. TOSCA¹⁵ instrument parameters assumed.

(FDS (16) at LANSCE, Los Alamos, USA) that the spectra were originally measured with. It can be seen that even though there are more modes present than would be the case if there was no coupling between the dihydrogen ligand and the other ligands, the pattern of the experimental spectrum is reproduced. The key result from the experimental difference spectrum is the determination of the dihydrogen torsional energy; the simulation shows that the first peak is largely due to this motion so this assignment is sound. However, location of the higher energy modes is much less certain.

The calculated ν_{th} of 3183 cm^{-1} is too high but this is the harmonic value, whereas the experimental value is an anharmonic value. This is also compounded by the tendency of DFT to overestimate frequencies.

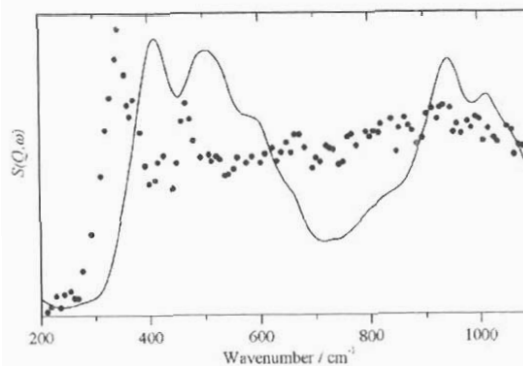


Figure 5. Comparison of experimental difference spectrum (points) of $[W(CO)_3(H_2)(P(iso-propyl)_3)_2]$ and the smoothed dihydrogen-only spectrum calculated from the DFT results.

Scaling the frequency by the usual value of 0.97 and assuming that the anharmonicity correction is 5.2% as for gaseous dihydrogen (17) gives a more reasonable value of 2926 cm^{-1} .

Inspection of the eigenvectors shows that the stronger modes generally agree with the literature assignments, Table 2. However, it is also apparent that the torsion, wag and rock are strongly coupled to the W=C=O linear bend deformation modes. This arises because as the heavy atoms move, to maintain the invariance of the centre-of-mass (a requirement for a normal mode) the hydrogens move in counterpoise. Since they are much lighter, a correspondingly larger amplitude of motion is required and this results in significant INS intensity. A similar effect is responsible for the intensity of the mode at 31 cm^{-1} , which rides the motion of the tungsten atom in the P-W-P equatorial bend

The mode at 360 cm^{-1} involves the wag, those at 386 , 425 and 648 cm^{-1} involve the rock and that at 457 cm^{-1} the torsion. A Wilson GF matrix method study of the cyclohexyl complex (14) came to similar conclusions, but considered that the

Table 2
Vibrational frequencies and intensities of dihydrogen in $[W(CO)_3(H_2)(P\{isopropyl\}_2)_2]$.

Mode	DFT ^a			Experimental ^{13,14}	
	Position / cm^{-1}	Infrared intensity / $km\ mol^{-1}$	Raman intensity / $\text{\AA}^4\ amu^{-1}$	Position / cm^{-1}	Infrared intensity ^b
ν_{HH}	3183	246	125	2690	s
ν_{HMH} asym	1495	50	13	1567	w
ν_{tMH} sym	940	135	64	953	m
Rock	585	11	3	660	-
Wag	522	5	11	465	w
Torsion	406	1	0	370/340	-

^aHarmonic values, ^bs = strong, m = medium, w = weak, - = not observed.

modes were coupled to the W-C stretches, which occur in the same region as the linear bends. This was done by introducing an interaction force constant between the relevant modes, whereas the DFT results suggest the hydrogen's response is a simple mechanical reaction.

The disadvantage of the vibrational model is that it is unable to account for the splitting in the modes, particularly the torsion. This is treated in an *ad hoc* fashion by recognising that the ground state is split by the tunnelling transition that results in the interchange of the two hydrogen atoms in the dihydrogen ligand. The tunnel splitting is present in all the vibrational levels and increases with increasing transition energy. We should remind the reader that the normal modes analysis is only valid for small displacements of the atoms around their equilibrium positions, and that rotations are not included, so their effects have to be a "bolt on" to the vibrational analysis.

Thus neither model is able to account for the spectrum without additional features being added. The reality is that both descriptions are valid but incomplete and how the intensity in the spectrum should be partitioned between the two models is a complex and, as yet, unresolved problem.

The difficulties with making assignments on the assumption that the dihydrogen modes are decoupled from the remainder of the molecule was also highlighted by a DFT analysis (18) of the $[Rh(H)_2(H_2)(Tp^{3,5-Me})]$ ($Tp^{3,5-Me} = (3,5\text{-dimethylpyrazolyl})\text{borate}$) complex. The original study (19) had assigned modes at 120 and 200 cm^{-1} as the transitions to the split torsional level. The DFT study showed that the 120 cm^{-1} modes were largely methyl torsions of the (3,5-dimethylpyrazolyl)borate ligand. For these to have appeared in the difference spectrum (H_4-D_4), the methyl torsions must be strongly coupled to (presumably) the dihydrogen torsion.

Our DFT results also allow us to assign the vibrational modes of the other ligands. The C=O stretches are calculated at 1798, 1810 and 1906 cm^{-1} with intensities of 1862000, 780000 and 42000 $m\ mol^{-1}$. After scaling the frequencies by the usual factor of 0.97, these are in good agreement, in both energy and relative intensity with the observed features (13) at 1852, 1867, and 1965 cm^{-1} . From the visualisation of the modes, these are assigned as the antisymmetric equatorial stretch, the axial stretch and the symmetric equatorial stretch respectively, although all three modes have all three carbonyl groups in motion. The three

modes can be considered as derived from the E and A modes of a C_{3v} $W(CO)_3$ fragment, where the degeneracy is lifted because of the C_1 symmetry. In the Raman spectrum of the cyclohexyl complex, whose frequencies are very close to those of the isopropyl complex, the most intense band is the highest energy mode, in agreement with the assignment of being derived from the totally symmetric mode of the hypothetical C_{3v} $W(CO)_3$ fragment.

The W–CO stretches and W–C=O linear angle bends occur in the 350 to 650 cm^{-1} range. Skeletal deformation modes of the isopropyl moieties also occur in this range. Visualisation of the modes allows the carbonyl modes to be identified. The same information that is used to generate the animations of the modes can be used in a different way. To generate the INS spectrum, the ACLIMAX program (7) calculates the amplitude of vibration of each atom from its displacement in each mode; the displacement is weighted by the total scattering cross section. If the cross sections of all the atoms are set to zero, except for the atom(s) of interest then the result shows which atoms have significant motion in each mode. This process was done separately for the carbon and oxygen atoms of the carbonyl ligands and the result is shown in Figure 6.

As expected, both atoms have motion in the same modes, although the amplitude are not always the same. For the W–CO stretches both carbon and oxygen have similar amplitudes since the CO is beating against the W, whereas for the W–C=O linear angle bends, the carbon has a much larger amplitude. The modes below 100 cm^{-1} are the CO–W–X bends, where X is either CO or P. In these the oxygen has a large amplitude of vibration because it is at the end of a long arm. The mode at 41 cm^{-1} is unusual; it consists of the central $W(CO)_3(H_2)$ unit rotating about the P–W–P axis with the phosphines moving in opposition.

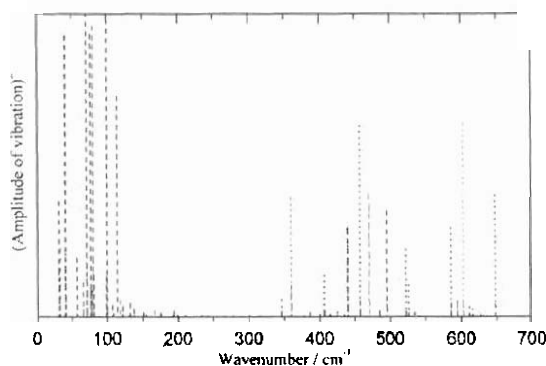


Figure 6. Amplitude of motion squared of the carbon atoms (dotted lines) and the oxygen atoms (dashed lines) of the carbonyl ligands of $[W(CO)_3(H_2)(P(iso-propyl))_3]_2$.

The C–H stretch and deformation modes are unremarkable and occur in the usual ranges (20). The methyl torsions are calculated at 192 to 266 cm^{-1} , again in the usual range (21). The W–P stretch and bend modes are highly mixed with the skeletal deformations of the alkyl groups. This is apparent from Figure 6, which shows the amplitude of vibration of the phosphorous atoms (dotted lines) and the alkyl carbon atoms (dashed lines). In the region below 700 cm^{-1} the similarity is striking, showing that both atoms are involved in the same modes. The lowest energy mode at 13 cm^{-1} is the counter-rotation of the two phosphine ligands accounting for its high intensity in both the total spectrum, Figure 4a, which is largely determined by the motions of the alkyl hydrogen atoms, and the carbon spectrum, Figure 6b. The axis of rotation is along the almost linear (178°) P–W–P chain, explaining why there is little motion of the phosphorus.

Conclusions

We have carried out a systematic investigation of the vibrational spectrum of the di-

hydrogen complex $[\text{W}(\text{CO})_3(\eta^2\text{-H}_2)(\text{P}(\text{isopropyl})_3)_2]$. Previous work has considered the motion of the dihydrogen ligand as either the rotational transitions of dihydrogen in a deep attractive well or as the modes of a conventional complex. We have shown that neither is able to account for the vibrational spectra, in particular the INS spectrum, on its own. The rotational model requires the addition of vibrations and the vibrational model requires the addition of a split ground state.

We have also shown that there is significant mechanical coupling of the dihydrogen modes to those of the other ligands present, especially the carbonyls. Simulation of the difference method used in the literature, shows that the most important INS result, the location of the torsional mode, is validated, but that the method is not reliable for higher energy modes.

The coupling of the dihydrogen to the other ligands means that there are no reliable group frequencies for the dihydrogen ligand. The most definitive mode is the H-H stretch, however, this is usually broad and weak, making it difficult to observe.

To date, there are no examples of dihydrogen ligated to a supported metal catalyst. However, there are tantalising hints that such species exist. Dihydrogen in Fe-ZSM (22) exhibits tunnel splittings of 4.2 and 8.3 cm^{-1} which are typical of the dihydrogen complexes. On the stepped surfaces of Ni(510) (23) and Pd(210) (24) after it is reacted with hydrogen to generate a dense atomic hydrogen layer, there is reasonable evidence that dihydrogen adsorbs intact at the steps. On the $\text{RuO}_2(110)$ surface, upon exposure at 85 K, H_2 weakly adsorbs as dihydrogen on coordinatively unsaturated ruthenium sites (25). The prospects seem good that chemisorbed dihydrogen will be observed on a supported metal surface and clearly vibrational spectroscopy would be an excellent tool for its investigation.

References

1. KUBAS G.J., RYAN R.R., SWANSON B.I., VERGAMINI, P.J., WASSERMAN, H.J. **J Am Chem Soc** 106: 451-452, 1984.
2. KUBAS G.J. **Metal dihydrogen and s-bond complexes**, Kluwer Academic, New York (USA), 2001.
3. KUBAS G.J. **J Organomet Chem** 635: 37-68, 2001.
4. HEINEKEY D.M., LLEDÓS A., LLUCH J.M. **Chem Soc Rev** 33: 175-182, 2002.
5. FRISCH M.J., TRUCKS G.W., SCHLEGEL H.B., SCUSERIA G.E., ROBB M.A., CHEESEMAN V.G., MONTGOMERY J.A.JR., VREVEN T., KUDIN K.N., BURANT J.C., MILLAM J.M., IYENGAR S.S., TOMASI J., BARONE V., MENNUECCI B., COSSI M., SCALMANI G., REGA N., PETERSSON G.A., NAKATSUJI H., HADA M., EHARA M., TOYOTA K., FUKUDA R., HASEGAWA J., ISHIDA M., NAKAJIMA T., HONDA Y., KITAO O., NAKAI H., KLENE M., LI X., KNOX J.E., HRATCHIAN H.P., CROSS J.B., ADAMO C., JARAMILLO J., GOMPERS R., STRATMANN R.E., YAZYEV O., AUSTIN A.J., CAMMI R., POMELLI C., OCHTERSKI J.W., AYALA P.Y., MOROKUMA K., VOTH G.A., SALVADOR P., DANNENBERG J.J., ZAKRZEWSKI V.G., DAPPRICH S., DANIELS A.D., STRAIN M.C., FARKAS O., MALICK D.K., RABUCK A.D., RAGHAVACHARI K., FORESMAN J.B., ORTIZ J.V., CUI Q., BABOULA G., CLIFFORD S., CIOŚLOWSKI J., STEFANOV B.B., LIU G., LIASHENKO A., PISKORZ P., KOMAROMI I., MARTIN R.L., FOX D.J., KEITH T., AL-LAHAM M.A., PENG C.Y., NANAYAKKARA A., CHALLACOMBE M., GILL P.M.W., JOHNSON B., CHEN W., WONG M.W., GONZALEZ C., POPE J.A. *Gaussian03* revision B.05 Gaussian Inc.: Pittsburgh PA 2003.
6. MITCHELL P.C.H., PARKER S.F., RAMIREZ-CUESTA A.J., TOMKINSON J. **Vibrational spectroscopy with neutrons with applications in chemistry biology materials science and catalysis** World Scientific Singapore (Singapore) 2005.

7. RAMIREZ-CUESTA A.J. *Comp Phys Comm* 157: 226-238, 2004.
8. LEVINE I.N. *Quantum Chemistry* 4th ed., Prentice-Hall: New Jersey (USA) 1991.
9. CELLI M., COLOGNESI D., ZOPPI M. *Phys Rev E* 66: 021202, 2002.
10. SMITH A.P., BENEDECK R., TROUW F.R., MINKOFF M., YANG L.H. *Phys Rev B* 53: 10187-10199, 1996.
ECKERT J., KUBAS G.J., HALL J.H., HAY P.J., BOYLE C.M. *J Am Chem Soc* 112: 2324-2332, 1990.
12. ECKERT J., KUBAS G.J. *J Phys Chem* 97: 2378-2384, 1993.
13. KUBAS G.J., UNKEFER C.J., SWANSON B.I., FUKUSHIMA E. *J Am Chem Soc* 108: 7000-7009, 1986.
BENDER B.R., KUBAS G.J., JONES L.H., SWANSON B.I., ECKERT J., CAPPS K.B., HOFF C.D. *J Am Chem Soc* 119: 9179-9190, 1997.
COLOGNESI D., CELLI M., CILLOCO F., NEWPORT R.J., PARKER S.F., ROSSI-ALBERTINI V., SACCHETTI F., TOMKINSON J., ZOPPI M. *Appl Phys A* 74: [Suppl.] S64-S66 2002.
16. TAYLOR A.D., WOOD E.J., GOLDSTONE J.A., ECKERT J. *Nucl Inst Meth Phys Res* 221: 408-418, 1984.
17. HERZBERG G. *Spectra of Diatomic Molecules* Van Nostrand Reinhold: New York (USA) 1950.
18. ECKERT J., WEBSTER C.E., HALL M.B., ALBINATI A., VENANZI L.M. *Inorg Chim Acta* 330: 240-249, 2002.
19. ECKERT J., ALBINATI A., BUCHER U.E., VENANZI L.M. *Inorg Chem* 35: 1292-1294, 1996.
20. LIN-VIEN D., COLTHUP N.B., FATELEY W.G., GRASSELLI J.G. *The Handbook of Infrared and Raman Characteristic Frequencies of Organic Molecules* Academic Press San Diego (USA) 1991.
21. BRADEN D.A., PARKER S.F., TOMKINSON J., HUDSON B.S. *J Chem Phys* 111: 429-437, 1999.
22. MOJET B.L., ECKERT J., VAN SANTEN R.A., ALBINATI A., LECHNER R.E. *J Am Chem Soc* 123: 8147-8148, 2001.. Evidence for chemisorbed molecular hydrogen in Fe-ZSM5 from inelastic neutron scattering.
23. MÅRTENSSON A.-S., NYBERG C., ANDERSSON S. *Phys Rev Lett* 53: 2045-2048, 1996.
24. SCHMIDT P.K., CHRISTMANN K., KRESE G., HAFNER J., LISCHKA M., GROSS A. *Phys Rev Lett* 87: 096103, 2001.
25. WANG J.H., FAN C.Y., SUN Q., REUTER K., JACOBI K., SCHEFFLER M., ERTL G. *Angew Chemie-Int Ed* 42: 2151-2154 2003.